Cell Reports, Volume *31*

Supplemental Information

Resolving Cell Cycle Speed in One Snapshot with a Live-Cell Fluorescent Reporter

Anna E. Eastman, Xinyue Chen, Xiao Hu, Amaleah A. Hartman, Aria M. Pearlman Morales, Cindy Yang, Jun Lu, Hao Yuan Kueh, and Shangqin Guo

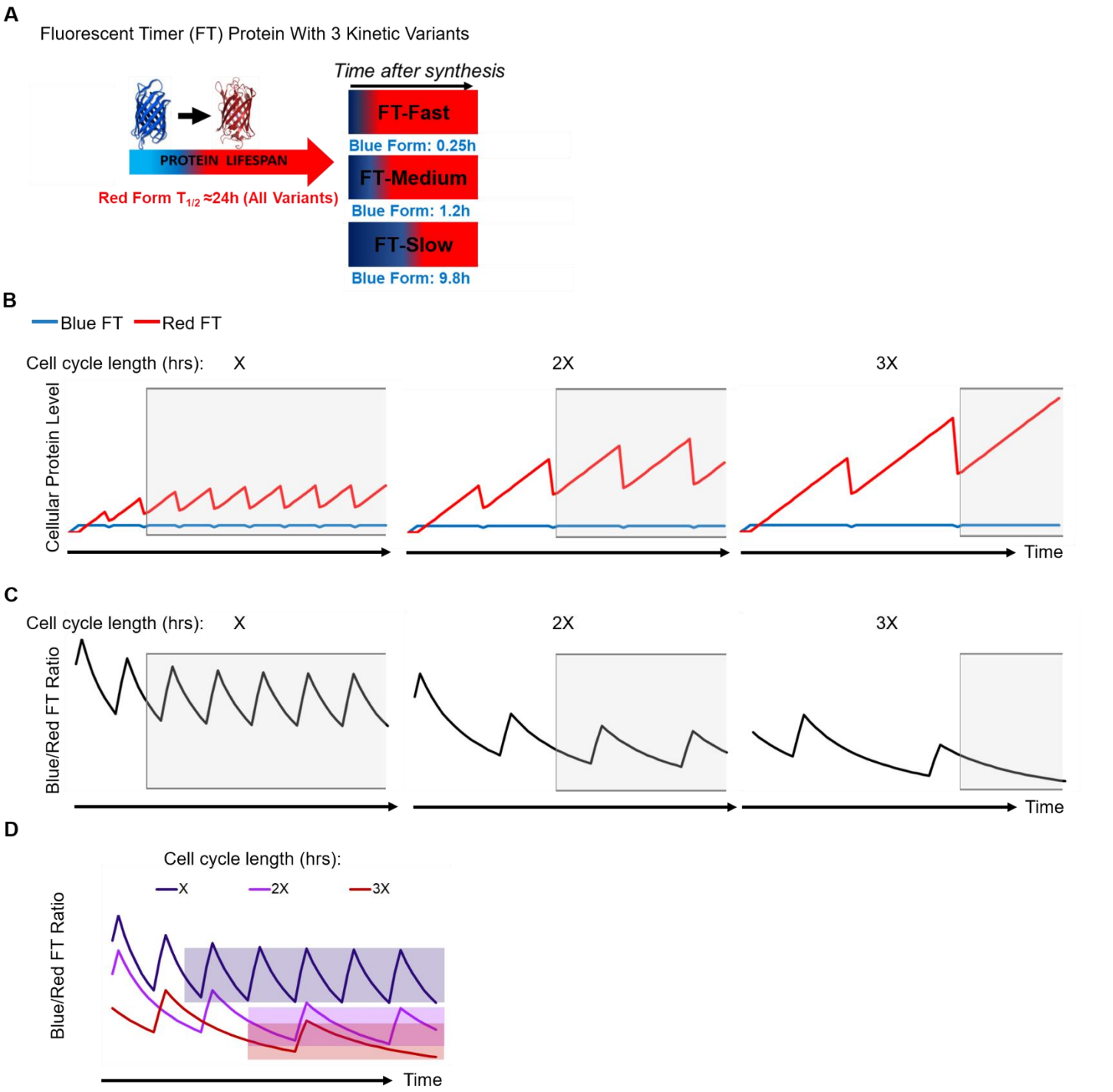

Figure S1 (Related to Figure 1). Modeling the dynamic behavior of FT fluorescence in relation to cell cycle length. A. The lifespan of the blue (immature) and red (mature) forms of the monomeric fluorescent timer (FT). Three kinetic variants were described by Subach et al. 2009. **B.** Results from mathematical modeling of blue and red FT levels following the onset of gene expression. Gray box shows the FT levels after reaching steady-state. Cells cycling at three distinct speeds are depicted: *X* (left), *2X* (middle) and *3X* (right) hours per cycle. Peaks/valleys represent maximum/minimum FT levels achieved before/after each mitosis. **C.** Blue/red FT ratio (BR) of cellular models from (B). **D.** Superimposed plots from (C). Shading indicates the area between the maximum and minimum BR for each cell cycle length, showing the anticipated separation of cells with different cell cycle lengths.

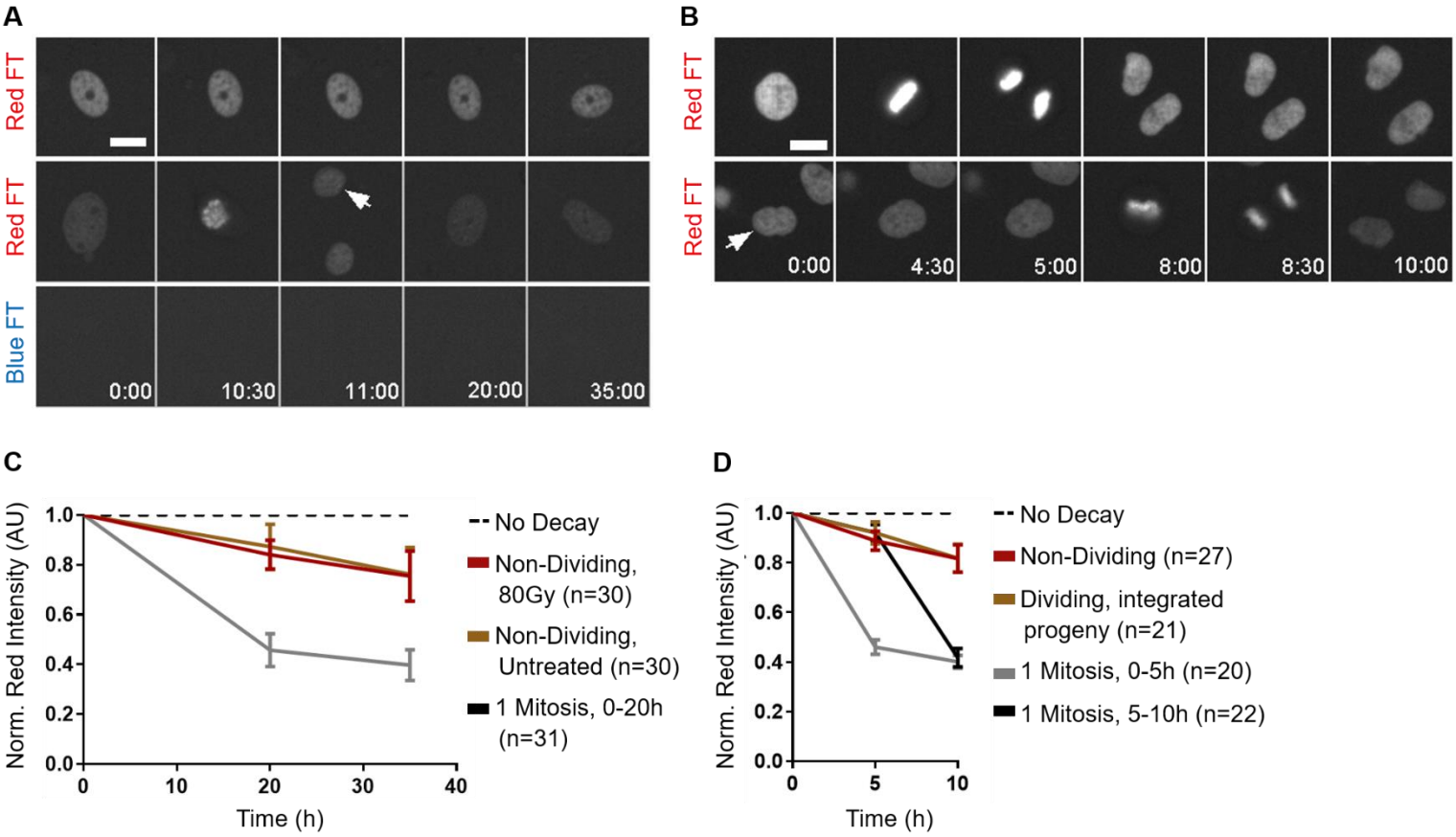

Figure S2 (Related to Figure 2). Characterization of H2B-FT-red decay in cultured cells. A. Representative time series of primary iH2B-FT MEF nuclei after Dox washout. Cells that never divided (top row) and cells that divided once (middle row) during the imaging period are shown. Images acquired in the blue channel (corresponding to the middle row, but representative of all regions) confirmed absence of new H2B-FT expression (bottom row). **B.** Representative time series of Hela nuclei after Dox washout. Cells that divided early (top row) and cells that divided late (bottom row) during the imaging period are shown. Arrows in (A-B) indicate which cell is followed in later timepoints. **C.** Quantification of the red FT in MEFs over time. Time 0 refers to the point when H2B-FT-blue signal fell below detection limit, due to complete conversion to red. **D.** Quantification of the red FT over time in Hela cells. When tracking the red fluorescence decay, the integrated red intensity measurements of all daughter nuclei were added together. Error bars denote SD; n refers to the number of single cells tracked per condition. Scale bars in (A-B)=20μm.

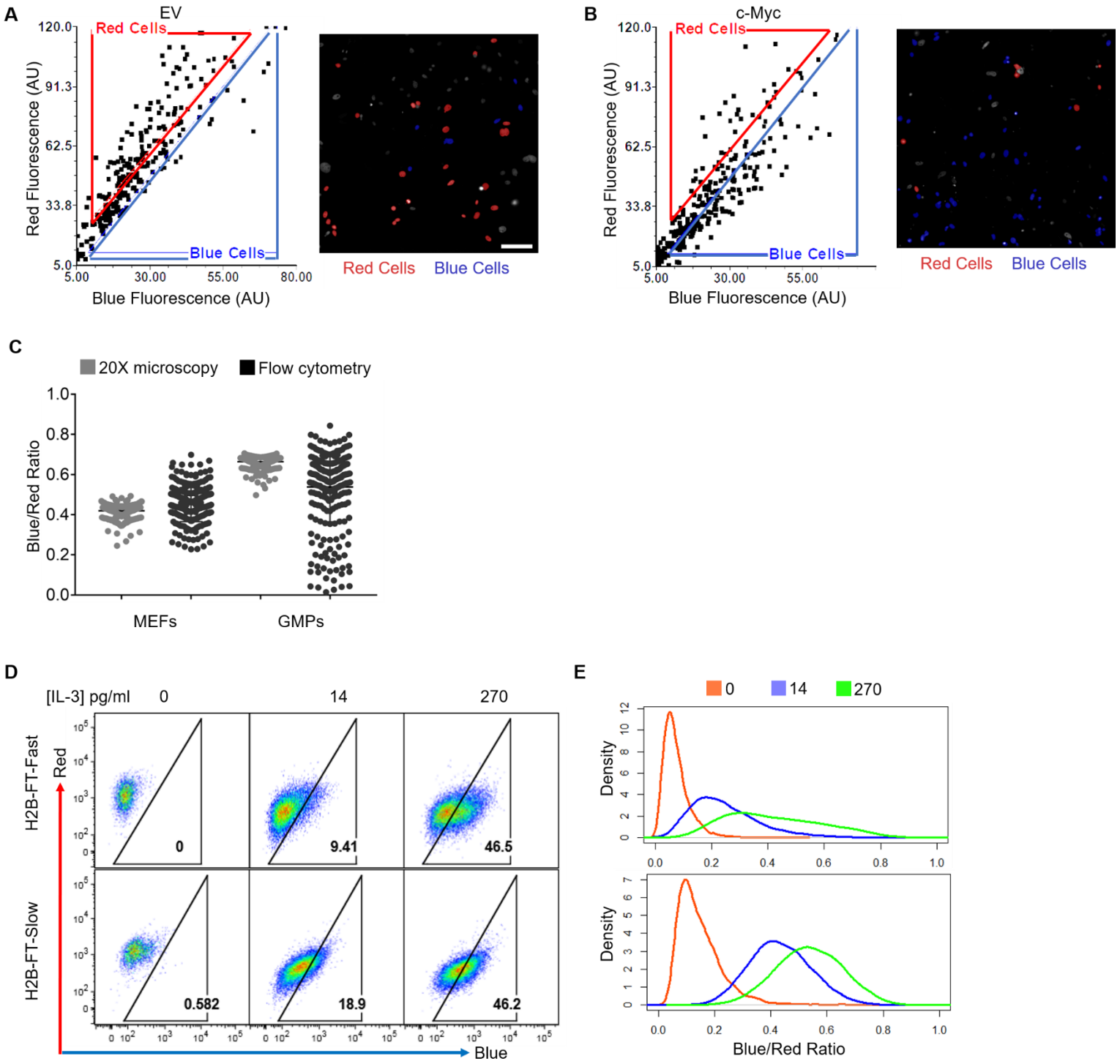

Figure S3 (Related to Figures 3-4). BR can be captured by microscopy or flow cytometry, and reflects proliferative changes *in vitro*. A-B. Image cytometry of MEFs transduced with either an empty control (A) or c-Myc overexpression vector (B) were captured by time-lapse microscopy for several days. Raw images were subjected to a quantitative processing workflow. Nuclear measurements of integrated red vs. blue fluorescence intensity were plotted for individual cells within each specific gate. Data from a representative well, combining four fields of view, are shown on the left. Representative fields of view of cells corresponding to the blue/red gating are shown on the right. Images are shown at the same scale. Scale bar=100µm. **C.** Comparison of BR dynamic range in MEFs and granulocyte-monocyte progenitors (GMPs) expressing H2B-FT-Medium as captured by live-cell 20X fluorescence microscopy (gray) vs. flow cytometry (black). **D.** Representative flow cytometry plots of BaF3 cells expressing H2B-FT-Fast (top) and H2B-FT-Slow (bottom) mutational variants, grown under different IL-3 concentrations. **E.** Flow cytometry data from (C) shown as density plots of BR.

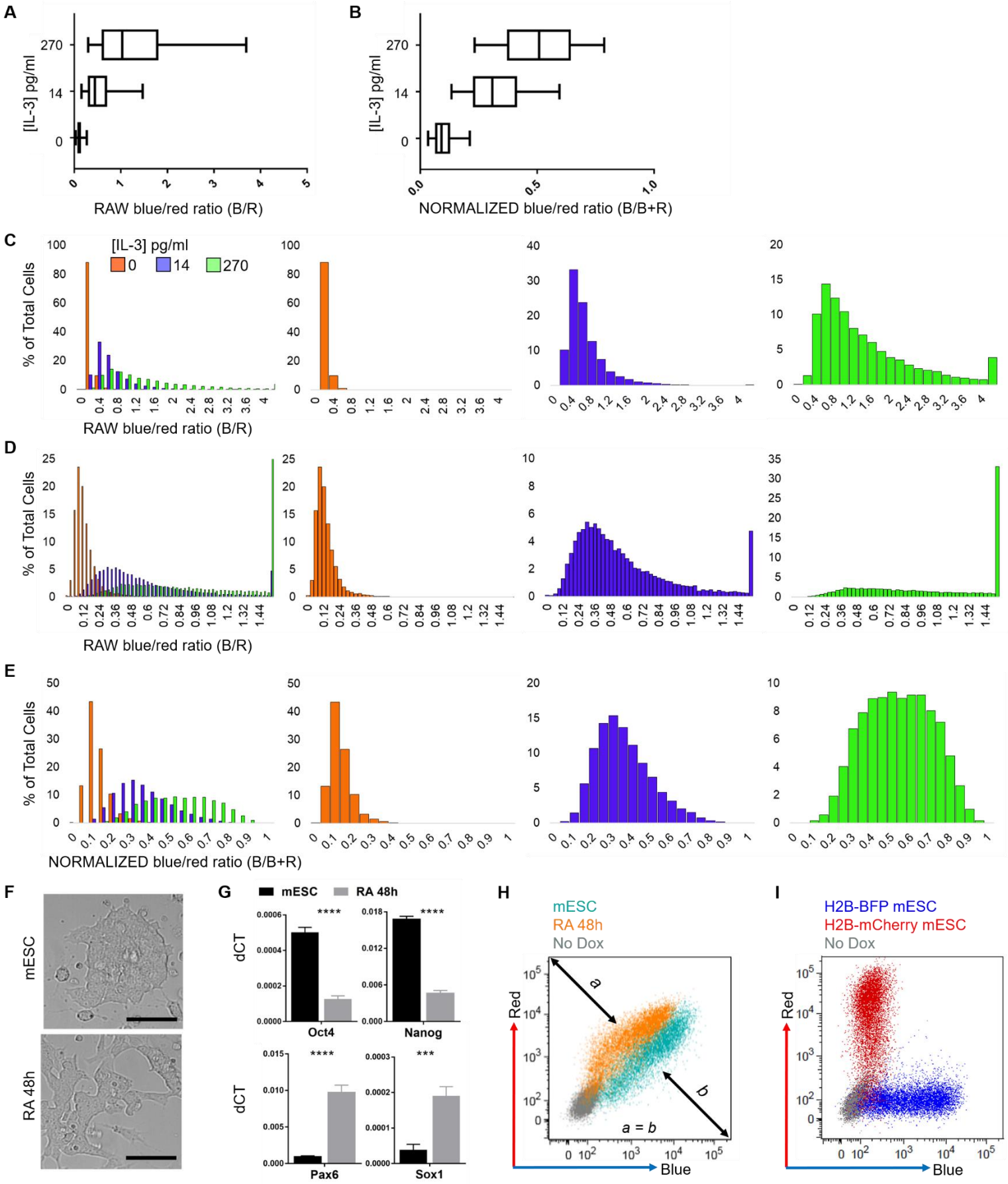

Figure S4 (Related to Figure 4). Validation of BR normalization and RA-induced mESC differentiation. (Legend on following page)

Figure S4 (Related to Figure 4). Validation of BR normalization and RA-induced mESC differentiation. A-B. Distributions of raw (A) vs. normalized (B) BR in BaF3 cells cultured in different concentrations of IL-3. **C-D**. Data from (A-B) displayed as histograms of raw BR. In panel (C), the binning strategy better depicts the dynamic range of bluer cells at the expense of the redder ones, while the opposite is true in (D). **E**. Data from (A-B) displayed as histograms of normalized BR, which equally depict both ends of the red-blue spectrum. For panels (A-B), the box plot represents the median and interquartile range of each group; whiskers represent 5th-95th percentile. **F.** Representative colony morphology of H2B-FT knock-in mESCs maintained in pluripotency maintenance conditions or following 48h RA treatment. Scale bars=80µm. **G**. RT-QPCR for pluripotency marker genes and early neuroectodermal genes. Error bars denote SD across n=3 replicate reactions. $P<0.0001$ (Oct4, Nanog, and Pax6) and $P=0.001$ (Sox1) determined using Student's T-Test with a 95% confidence interval, dF=4. **H.** Benchmark for establishing flow cytometry voltage settings to analyze cells expressing H2B-FT-Medium: blue vs. red flow cytometry profile of H2B-FT-Medium pluripotent and RA-treated mESCs, as shown in Figure 4F. Diagonal lines of equal length have been drawn onto the figure to emphasize that H2B-FT-expressing populations should be centered in 2D between the blue and red axes for best resolution of BR. **I.** The voltage settings in (H) were determined using a colorless sample (H2B-FT knock-in mESCs not exposed to Dox) and single-color cell lines (H2B-BFP and H2B-mCherry knock-in mESCs for blue and red, respectively). For the H2B-FT-Medium variant, optimal voltage settings place the brightest H2B-BFP population between $10^3 – 10^4$ and the brightest H2B-mCherry population between $10^4 – 10^5$. Note that blue and red axes are displayed on the same scale.

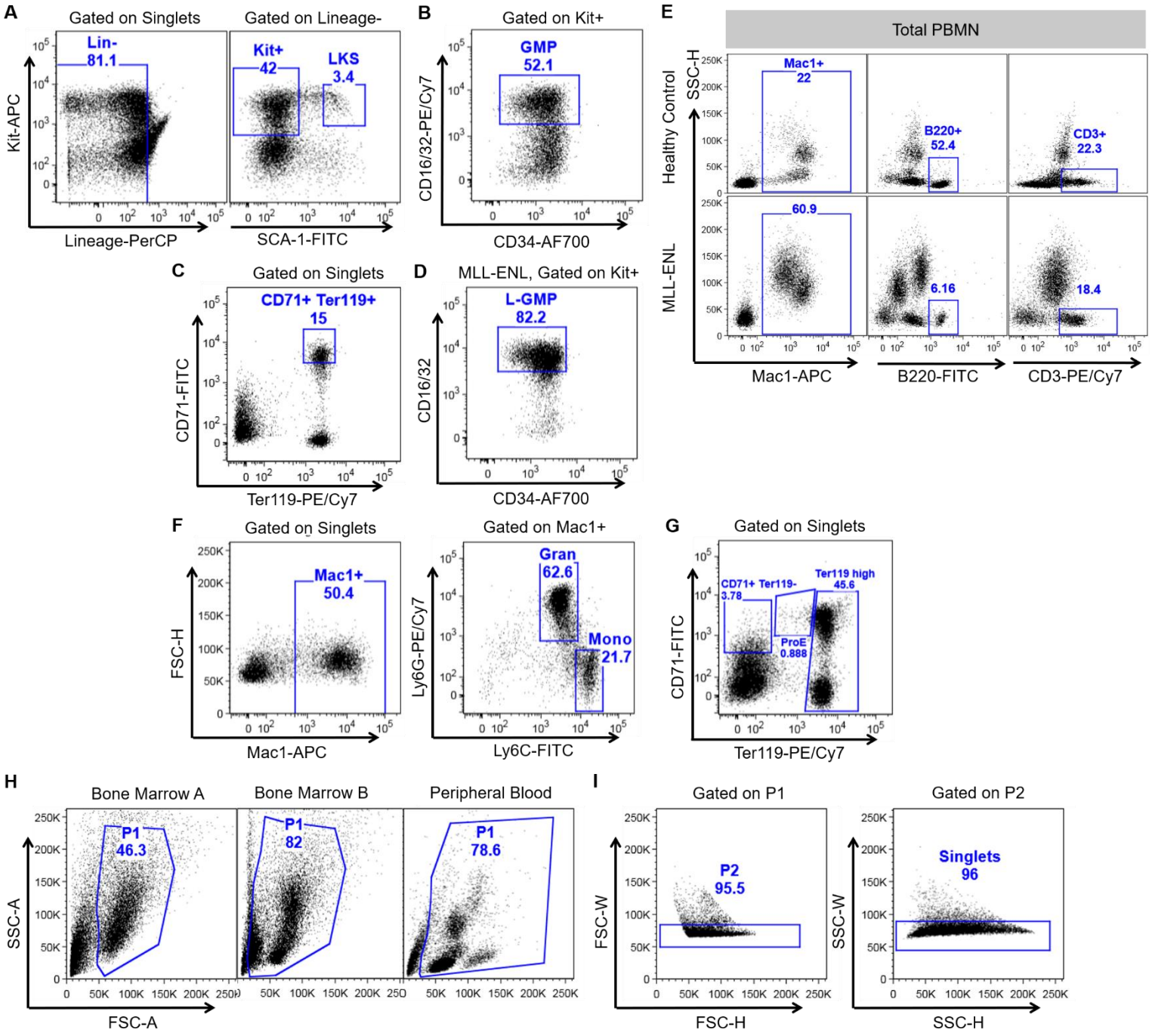

Figure S5 (Related to Figure 5). Identification of specific hematopoietic populations in bone marrow and peripheral blood. A-B. Gating for LKS and GMP. **C.** Gating for CD71+/Ter119+ erythroid cells. **D.** Gating for L-GMP compartment from H2B-FT x iMLL-ENL mice following 8d Dox treatment. **E.** Myeloid (Mac1+), B-cell (B220+), and T-cell (CD3+) compartments in peripheral blood mononuclear (PBMN) cells of healthy H2B-FT mice (top) and H2B-FT x iMLL-ENL mice following 8d Dox treatment (bottom). **F.** Gating for bone marrow monocytic and granulocytic cells. **G.** Gating strategy for distinct stages of erythroid differentiation. **H.** Initial determination of live cells by forward- and side-scatter gating. All bone marrow populations (A-D, F) were gated as shown in "Bone Marrow A", except for erythroid cells (G) which were gated as shown in "Bone Marrow B". PBMN (E) were gated as shown in "Peripheral Blood". **I.** Doublet exclusion strategy used for all bone marrow and PBMN populations.

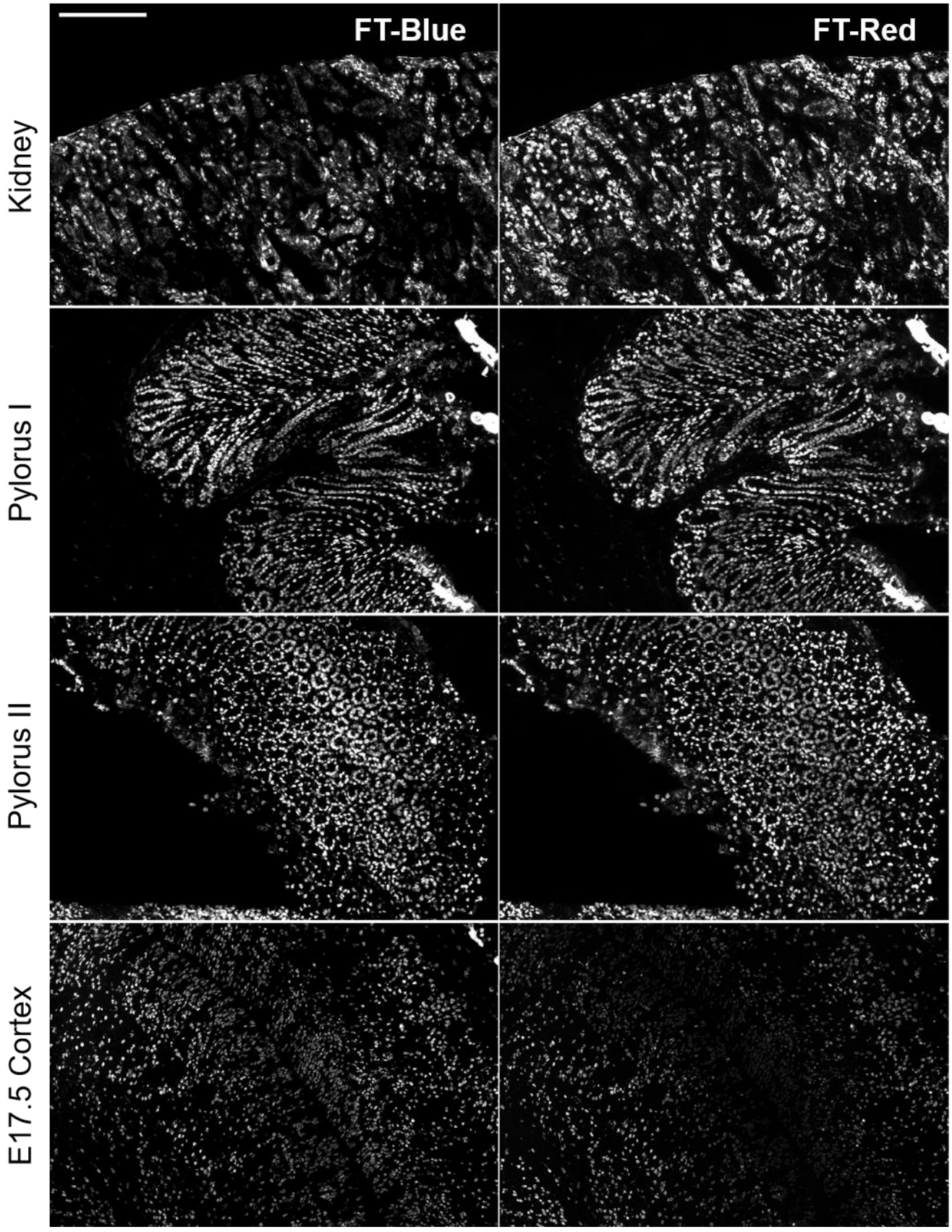

Figure S6 (Related to Figure 6). H2B-FT color profile is consistent with relative turnover rates in solid tissue sections. Single-channel fluorescence images showing H2B-FT-Blue and H2B-FT-Red in solid tissue sections. Kidney (top) and pylorus in two orientations (middle) from a representative adult iH2B-FT mouse are shown. Bottom, the neocortex of a representative E17.5 iH2B-FT mouse embryo. Scale bar=200μm.

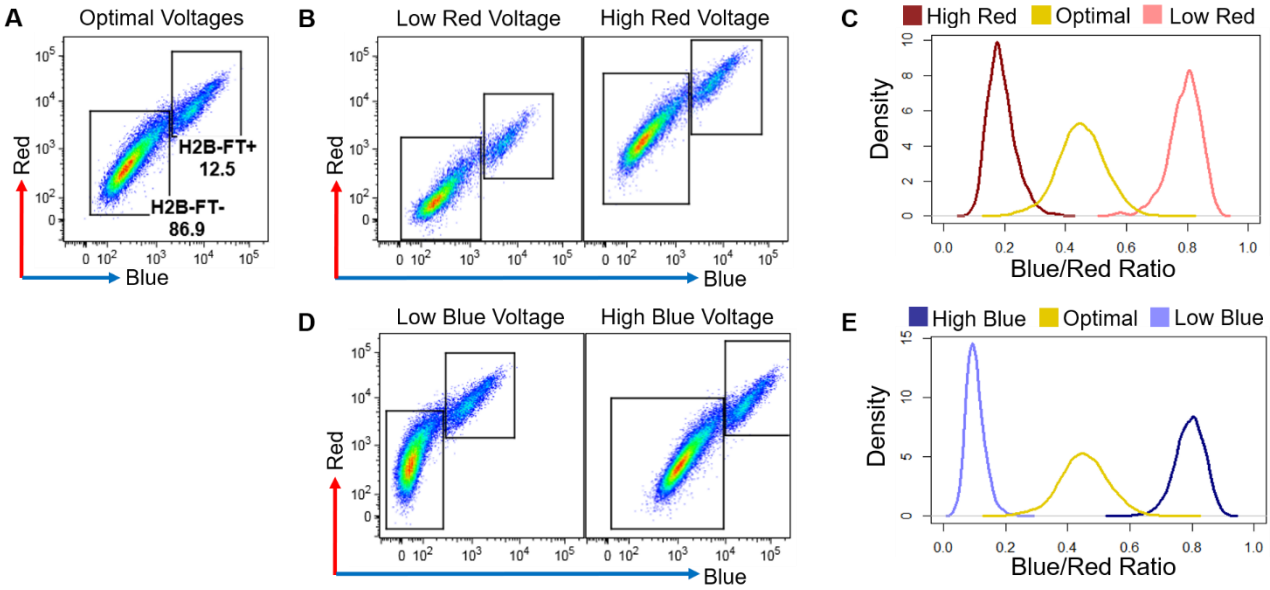

F

Equation S2b:

$$\frac{\bar{B}}{\bar{R}} = \frac{C \cdot \tau_C}{\tau_D}$$

Equation S2b, Normalized:

$$\frac{\bar{B}}{\bar{B} + \bar{R}} = \frac{C \cdot \tau_C}{C \cdot \tau_C + \tau_D}$$

G

CC length percentile	Actual CC length (h)	Blue/red ratio percentile	Blue/red ratio value	Derived $C \cdot \tau_C$ Value	Prediction 1: CC length (h)	Prediction 2: CC length (h)	Prediction 3: CC length (h)	Prediction 4: CC length (h)
10	9.12	90	0.711	**22.44**	**9.12**	8.19	7.95	7.06
25	10.7	75	0.653	**20.14**	11.92	**10.70**	10.40	9.23
50	14	50	0.583	**19.57**	16.05	14.41	**14.00**	12.42
80	21.4	20	0.448	**17.37**	27.65	24.82	24.11	**21.40**

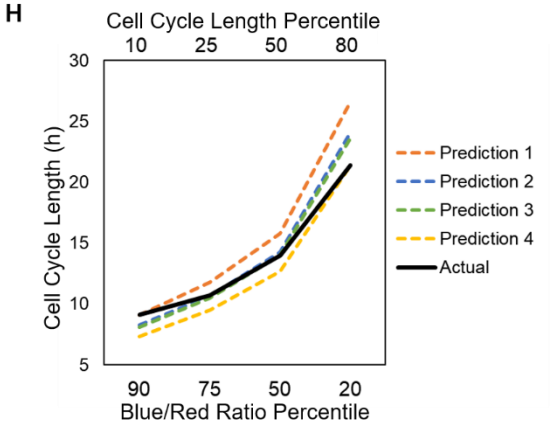

I

Equation S2d:

$$\frac{\bar{B}}{\bar{R}} = C \cdot \tau_C \left(\frac{1}{\tau_D} + \frac{1}{\tau_R}\right)$$

Equation S2d, Normalized:

$$\frac{\bar{B}}{\bar{B} + \bar{R}} = \frac{C \cdot \tau_C}{C \cdot \tau_C + (\frac{1}{\tau_D} + \frac{1}{\tau_R})^{-1}}$$

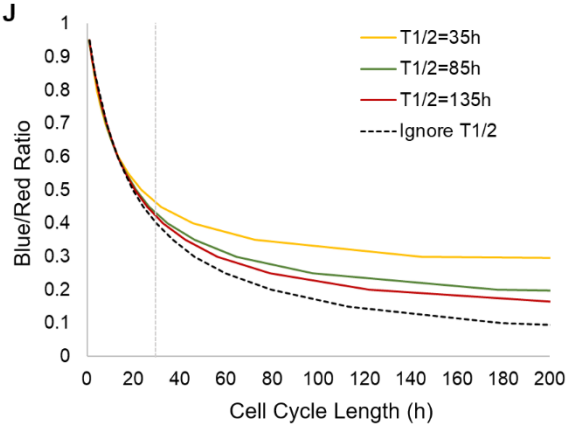

K

Blue/Red Ratio	Calculated CC Length (h) Given by Red $T_{1/2}$ = 35h	Calculated CC Length (h) Given by Red $T_{1/2}$ = 85h	Calculated CC Length (h) Given by Red $T_{1/2}$ = 135h	CC Length, Mean of 3 Calculations	Error Range (h)
0.25	1013.91	97.61	79.09	396.87	934.8
0.3	144.37	64.51	56.42	88.43	88.0
0.35	72.57	46.37	42.40	53.78	30.2
0.4	45.92	34.91	32.87	37.90	13.1
0.45	32.02	27.02	25.97	28.34	6.1
0.5	23.49	21.26	20.75	21.83	2.7
0.55	17.72	16.86	16.65	17.08	1.1
0.6	13.56	13.40	13.36	13.44	0.2
0.65	10.41	10.60	10.65	10.55	0.2
0.7	7.95	8.29	8.38	8.21	0.4
0.75	5.98	6.35	6.46	6.26	0.5
0.8	4.35	4.70	4.80	4.62	0.4
0.85	3.00	3.28	3.37	3.22	0.4
0.9	1.85	2.05	2.11	2.00	0.3
0.95	0.86	0.96	0.99	0.94	0.1

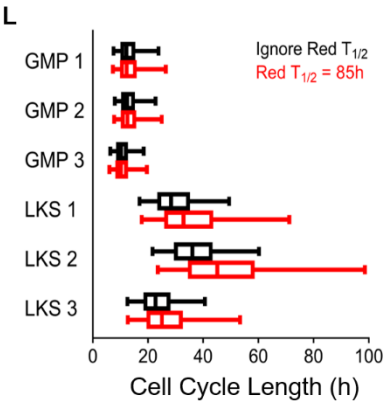

Figure S7 (Related to Figure 7). Determining critical parameters for calculating cell cycle length from BR. (Legend on following page)

Figure S7 (Related to Figure 7). Determining critical parameters for calculating cell cycle length from BR. A. Flow cytometry plot showing the red vs. blue color profile of primary MEFs expressing H2B-FT. "Optimal" voltage settings were carefully determined using single-color controls and all-negative controls. Altering fluorescence detection parameters impacts the BR dynamic range as follows: **B.** The same sample as in (A) analyzed using lower (left) or higher (right) detection voltages for the red fluorescence. **C.** BR distributions of flow cytometry data from (A-B). **D.** The same cells as in (A-C) analyzed using lower (left) or higher (right) detection voltages for the blue fluorescence. **E.** BR distributions of flow cytometry data from (A) and (D). **F**. The mathematical model detailed in Data S2 predicts that cell cycle length can be determined from the steady-state BR of cells expressing H2B-FT. Since red molecules are stable, the rate of red removal (δ) can be simplified to be inversely proportional to the cell cycle time (τ_D). τ_C is the blue-to-red conversion time and *C* is a normalization constant. The equation can also be solved using the normalized BR value, B/(B+R). **G.** Four paired data points of corresponding cell cycle (CC) length percentile and BR percentile (as shown in Figure 7A-B) were used to derive the $C \cdot \tau_C$ value using the equation in (F). Each $C \cdot \tau_C$ value (shown in bold) was then applied onto the other three BR values to generate four separate predictions of cell cycle lengths. Bold cell cycle lengths indicate the experimentally observed value. **H.** The four predicted cell cycle length curves were compared with the actual data (solid black line). From this plot, a $C \cdot \tau_C$ value representing the average of predictions 2 and 3 was selected for estimating *in vivo* cell cycle lengths. **I**. The equation was modified to incorporate a rate constant, τ_R, for active protein degradation. τ_R is related to protein half-life via the formula $T_{1/2} = \tau_R \cdot \ln 2$. **J**. The effect of red half-life on the quantitative model relating BR and cell cycle length. Since the value of the H2B-FT-Red half-life *in vivo* is currently unknown, we derived curves using the formula in (I) by inputting various half-life values ranging from 35-135h. Black lines in each plot show the curve obtained using the simplified version of the equation in Data S2 (F), in which red decay is ignored. Vertical dotted gray line shows the distance between the predictions at cell cycle length = 30h. **K.** The difference (h) in cell cycle lengths calculated from a range of BR values when H2B-FT-Red half-life varies from 35h (similar to that in Hela cells, see Figure S2D), to 85h (similar to that in MEFs, see Figure S2C) and to 135h. **L.** Cell cycle length distributions of LKS and GMP populations from three mice (as in Figure 7F) calculated using different red fluorescent half-life parameters. Boxes represent the median and IQR; whiskers represent 5th-95th percentile.

Experimental Considerations for the H2B-FT Reporter	
H2B-FT expression	Stable and sustained H2B-FT expression should precede analysis. This is to guard against BR changes due to nascent or ceasing reporter expression. If using Dox-inducible promoter, Dox should be added for ≥1 week prior to analysis (longer for slow-turnover tissues).
Excitation/emission spectra	Choose appropriate filter/LED or filter/laser combinations that match the excitation/emission spectra of FT-Blue and FT-Red (Subach et al., 2009). BFP/mCherry have similar spectra to FT-Blue/FT-Red and are good single-color controls.
Signal-to-noise ratio (SNR) Observe best practices for maximizing fluorescent protein SNR.	Always include negative controls of the same tissue or cell type being analyzed. H2B-FT+ cells should be clearly distinguishable from negative controls without oversaturation. Microscopy: When possible, capture solid tissue sections in an empty channel, such as green, for subtracting autofluorescence. Minimize sample thickness and maximize spatial resolution.
Balancing blue and red signal	Evaluate balance by rendering raw data into normalized BR (B/(B+R)), where B and R refer to integrated cellular intensity in blue (B) and red (R) channels. Plot the distribution on a 0-1 scale. Optimal setting should yield a centered major peak, shown in Figure S7A-E. Flow cytometry: Adjust voltage settings to center H2B-FT+ population between blue and red axes, shown in Figure S4H and Figure S7A,C,E. H2B-BFP and H2B-mCherry expressing cell lines are helpful for calibrating voltages, shown in Figure S4I.
Photosensitivity of FT-Blue UV or violet light exposure causes premature color change of FT-Blue.	Microscopy: Acquire red channel before blue for each frame. For time-lapse, image blue channel less frequently. Capture other channels more frequently if needed for cell tracking. Avoid repeated UV exposures; use widefield instead of confocal microscopy; scan tile regions with 0% overlap; test settings on a dispensable region.
Fluorescence multiplexing	Single-color controls should be used to determine spectral bleed-through into blue and red channels. Microscopy: Mitigate spillover through careful choice of filters; choose fluorophores that are most compatible with H2B-FT; reduce staining concentration; or (when possible) stain and re-acquire samples after capturing BR. Flow cytometry: H2B-BFP and H2B-mCherry cell lines are useful single-color controls for auto-generated compensation, which should be manually adjusted since BFP and mCherry are brighter than FT-Blue and FT-Red, respectively.
Temperature	The FT blue-to-red conversion rate is temperature-dependent (Subach et al. 2009). Keep samples on ice during processing to preserve native BR for analysis.
Sample preservation	Chemical fixation destroys FT-Blue. Always acquire H2B-FT fluorescence prior to fixation and downstream staining. Microscopy: Flash-freezing preserves tissue specimens and H2B-FT fluorescence. Flow cytometry: Live cells can be sorted on BR by fluorescence activated cell sorting and fixed afterward for intracellular staining.
Quantitative estimation of cell cycle length	Flow cytometry is the preferred detection method for deriving quantitative estimate of cell cycle length due to its superior sensitivity. Qualitative or relative differences in cell cycle speed can be obtained by all fluorescence detection methods. Cell cycle length quantification requires calibration with a cell type whose median cell cycle length is known: BR must be measured on the same instrument used to acquire samples of unknown cycling rate. Cell size and morphology of the calibration sample should also be similar to the cell type being studied.

Table S1 (Related to STAR Methods). Experimental considerations for working with the H2B-FT reporter in microscopy and/or flow cytometry assays.

Cloning	**Sequence (5'-3')**
Gateway *FT-Fast/Slow* Fwd	GGGGACAACTTTGTACAAAAAAGTTGCCACCATGGTGAGCAAGGGCGAG
Gateway *FT-Medium* Fwd	GGGGACAACTTTGTACAAAAAAGTTGCCACCATGGTAAGCAAGGGCGAG
Gateway *FT-Fast/Slow* Rev	GGGGACAACTTTGTACAAGAAAGTTGGCAATTACTTGTACAGCTCGTCCATG
Gateway *H2B* Fwd	GGGGACAACTTTGTACAAAAAAGTTGGCACCATGCCAGAGCCAGCGAAGTCT
H2B-FT-Fast/Slow Junction Fwd	AGCGCTAAGGATCCGATGGTGAGCAAGGGCGAGGAGGATAA
H2B-FT-Fast/Slow Junction Rev	ACCATCGGATCCTTAGCGCTGGTGTACTTGGTGACGGCCTTA
H2B-FT-Medium Junction Fwd	AGCGCTAAGGATCCGATGGTAAGCAAGGGCGAGGAGGATAA
pSCMV *FT-Fast/Slow* Fwd	TATTAAGCTTGCCACCATGGTGAGCAAGGGCGAGGA
pSCMV *FT-Medium* Fwd	TATTAAGCTTGCCACCATGGTAAGCAAGGGCGAGGA
pSCMV *FT-Fast/Medium/Slow* Rev	CCGTCTCGAGTTACTTGTACAGCTCGTCCATGCC
pSCMV and p2lox *H2B* Fwd	TATTAAGCTTGGCACCATGCCAGAGCCAGCGAA
p2lox and pT3 *FT-Fast/Medium/Slow* Rev	CCGTGCGGCCGCTTACTTGTACAGCTCGTCCAT
pT3 *MCS* Fwd	CGCGTGGCGCGCCTTAATTAAGTTTAAACGC
pT3 *MCS* Rev	GGCCGCGTTTAAACTTAATTAAGGCGCGCCA
pT3 *H2B* Fwd	GTATTGTTTAAACGGCACCATGCCAGAGCCAGCGAA
Genotyping	
HPRT::H2B-FT Knock-in Fwd	CTAGATCTCGAAGGATCTGGAG
HPRT::H2B-FT Knock-in Rev	ATACTTTCTCGGCAGGAGCA
HPRT::H2B-FT WT Fwd	GTCATAGGAACTGCGGTCGT
HPRT::H2B-FT WT Rev	GCTGGGATTTGAACTCAGGA
Rosa26::rtTA WT Fwd	AAAGTCGCTCTGAGTTGTTAT
Rosa26::rtTA rtTA FWD	GCGAAGAGTTTGTCCTCAACC
Rosa26::rtTA Rosa26 Rev	GGAGCGGGAGAAATGGATATG
Col1::MLL-ENL Col1 Fwd	TCCCTCACTTCTCATCCAGATATT
Col1::MLL-ENL Knock-in Rev	GGACAGGATAAGTATGACATCATCAA
Col1::MLL-ENL WT Rev	AGTCTTGGATACTCCGTGACCATA
qPCR	
Oct4 Fwd	TCTTTCCACCAGGCCCCCGGCTC
Oct4 Rev	TGCGGGCGGACATGGGGAGATCC
Nanog Fwd	AAATCCCTTCCCTCGCCATC
Nanog Rev	TTTGGGACTGGTAGAAGAATCAGG
Pax6 Fwd	ACCAGTGTCTACCAGCCAATCC
Pax6 Rev	GCACGAGTATGAGGAGGTCTGA
Sox1 Fwd	GCCGAGTGGAAGGTCATGTC
Sox1 Rev	TTGAGCAGCGTCTTGGTCTTG
GAPDH Fwd	GGTGCTGAGTATGTCGTGGAG
GAPDH Rev	GGCGGAGATGATGACCCTTT

Table S2 (Related to STAR Methods). Primer sequences used for cloning, genotyping, and qPCR.

A

Here, we derive mathematical expressions for differences in the level of a molecule *M* between two cell populations, one with a shorter cell cycle time τ_1, and another with a longer cell cycle time τ_2. The dynamical equations describing the time evolution of this system are given by:

$$\frac{dM_1}{dt} = k_1 - \left(\frac{1}{\tau_1} + \frac{1}{\tau_P}\right) M_1 \quad (1)$$

$$\frac{dM_2}{dt} = k_2 - \left(\frac{1}{\tau_2} + \frac{1}{\tau_P}\right) M_2 \quad (2)$$

where M_1 and M_2 give the levels of the molecules in the two cell populations, k_1 and k_2 give its synthesis rates in the two populations respectively, and τ_P gives its time constant for degradation, which is assumed to be the same in the two populations. Solving for the steady-state level of the molecular species in the system, we have that:

$$M_1 = k_1 \tau_1 \left(\frac{\sigma_P}{\sigma_P + 1}\right) \quad (3)$$

where $\sigma_P = \tau_P/\tau_1$ is the ratio of the molecular half-life to the cell cycle duration of the first cell population. Similarly,

$$M_2 = k_2 \tau_2 \left(\frac{\sigma_P}{\sigma_P + \sigma_2}\right) \quad (4)$$

where $\sigma_2 = \tau_2/\tau_1 > 1$ is the ratio of the cell cycle duration of the second population to that of the first populations. From these two equations, we find that the ratio of the molecule levels of the slow cycling population to that of the fast-cycling population is given by:

$$\mu = \frac{\kappa\, \sigma_2(\sigma_P + 1)}{(\sigma_P + \sigma_2)} \quad (5)$$

where $\kappa = k_2/k_1$ is the ratio of synthesis rates for the slow versus fast-cycling populations.

From this expression a few features are apparent: 1) when the molecule is extremely unstable compared to the cell cycle time ($\sigma_P \ll 1$), this ratio converges to the ratio of synthesis rates between the two populations κ. 2) When the molecule half-life is much longer than the longer cell cycle length $\sigma_P \gg \sigma_2$, this ratio is now given by the synthesis rates multiplied by the ratio of the long cell-cycle length to the short cell cycle length $\kappa\sigma_2$. Thus, when synthesis rates of the two populations are the same, relative differences in the abundance of this molecule are simply given by the relative differences in cell cycle lengths between these two populations. When synthesis rates of two populations are different ($\kappa \neq 1$), cell cycle length differences amplify these differences by a constant multiplicative factor. 3) As the half-life of the molecule increases, relative differences in its levels increase, and reach a half-maximum when its half-life is equal to the longer cell cycle length ($\sigma_P = \sigma_2$; see black dot in (b)).

B

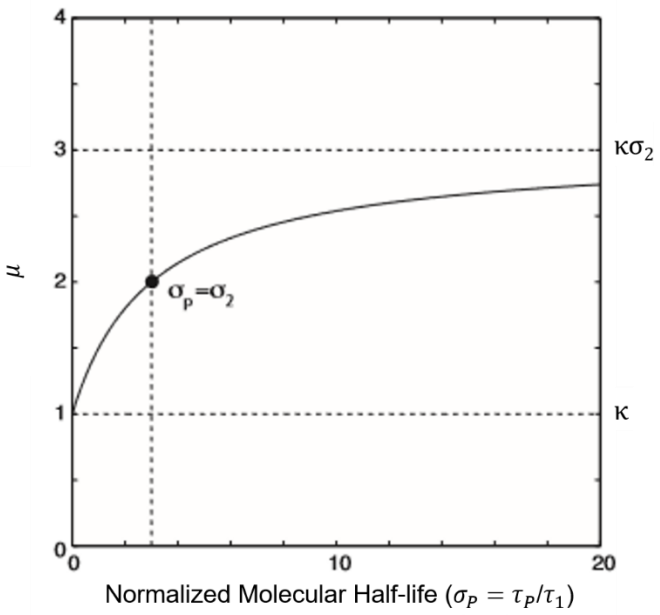

Data S1 (Related to Figure 1). A molecule's intracellular level depends on the molecule's half-life and cell cycle length. A. Equation describing the ratio (μ) of levels of a molecule (*M)* in two populations of cells with different cell cycle lengths. $\sigma_2 = \tau_2/\tau_1 > 1$ is the ratio of cell cycle lengths; $\sigma_P = \tau_P/\tau_1$ is the ratio of the molecule's half-life to the shorter cell cycle length; and $\kappa = k_2/k_1$ is the ratio of the molecule's synthesis rates between the two cell populations. **B.** Graph of μ values illustrating the dependence of molecule levels on the half-life and cell cycle length. Parameters: $\kappa = 1$, and $\sigma_2 = 3$. Note that levels of molecules at which this ratio is half-maximal is given by the black dot ($\sigma_P = \sigma_2$).

A

The levels of stable fluorescent proteins are strongly influenced by cell division, which results in their removal by dilution. We can exploit this concept to generate a live-cell reporter of cell cycle speed, using a color-changing fluorescent timer protein. The following ordinary differential equations describe the time evolution of such a timer:

$$\frac{dB}{dt} = \alpha - \frac{B}{\tau_C} \quad (1)$$

$$\frac{dR}{dt} = \beta B - \delta R \quad (2)$$

Here *B* is the blue emitting initial molecular species, *R* is the red-emitting molecular species after fluorescence conversion, α is the synthesis rate, τ_C is the time constant for fluorescence conversion, and δ is the rate of protein removal. In the most general case, the rate of protein removal is a sum of the rates of proteasomal degradation and cell division; however, when the fluorescent protein is stable, this parameter is simply inversely proportional to the cell cycle time τ_D:

$$\delta = 1/\tau_D \quad (3)$$

Solving for the steady state of the system, we find that:

$$\bar{B} = \tau_C \alpha \quad (4)$$

$$\bar{R} = \alpha/\delta \quad (5)$$

Consequently, we find that the observed steady-state ratio of the two quantities;

$$\frac{\bar{B}}{\bar{R}} = C \cdot \tau_C \left(\frac{1}{\tau_D}\right) \quad (6)$$

where *C* is a normalization constant.

B

$$\frac{\bar{B}}{\bar{R}} = \frac{C \cdot \tau_C}{\tau_D}$$

C

The rate of protein removal, δ, can be expanded in scope to include active degradation in addition to cell-division-dependent dilution. When both processes are active:

$$\delta = 1/\tau_R + 1/\tau_D \quad (3.1)$$

where τ_D is cell division time, and τ_R is the time constant for active degradation. Solving for the steady state of the system, we find that:

$$\bar{B} = \tau_C \alpha \quad (4)$$

$$\bar{R} = \alpha/\delta \quad (5)$$

Consequently, we find that the observed steady-state ratio of the two quantities;

$$\frac{\bar{B}}{\bar{R}} = C \cdot \tau_C \left(\frac{1}{\tau_D} + \frac{1}{\tau_R}\right) \quad (6.1)$$

where *C* is a normalization constant.

D

$$\frac{\bar{B}}{\bar{R}} = C \cdot \tau_C \left(\frac{1}{\tau_D} + \frac{1}{\tau_R}\right)$$

Data S2 (Related to Figure 1). Relationship between FT blue/red ratio (BR) and cell cycle length. A. The steady-state levels of the blue and red forms of the FT ($\bar{B}$ and $\bar{R}$, respectively) are the net result of protein synthesis rate (*α*) and turnover rate. Blue turnover (*β*) happens upon conversion from blue to red after a period of time (τ_C). Since red molecules are stable, the rate of red removal (*δ*) can be understood to be inversely proportional to the cell cycle time (τ_D). *C* is a normalization constant. **B.** Taken together, a simplistic estimation of cell cycle length can be determined from the steady-state blue/red ratio or vice-versa. **C-D.** A modified version of the equation incorporates a rate constant, τ_R, for active protein degradation. τ_R is related to protein half-life via the formula $T_{1/2} = \tau_R \cdot ln2$.